Letter

Current-induced brightening of vacancy-related emitters in hexagonal boron nitride

Corinne Steiner,[1,2,*] Rebecca Rahmel,[1] Frank Volmer,[1,3] Rika Windisch,[4] Lars H. Janssen,[1] Patricia Pesch,[1] Kenji Watanabe,[5] Takashi Taniguchi,[6] Florian Libisch,[4] Bernd Beschoten,[1] Christoph Stampfer,[1,2] and Annika Kurzmann[1,7,†]

[1]*JARA-FIT and 2nd Institute of Physics, RWTH Aachen University, 52074 Aachen, Germany*
[2]*Peter Grünberg Institute (PGI-9), Forschungszentrum Jülich, 52425 Jülich, Germany*
[3]*AMO GmbH, Advanced Microelectronic Center Aachen (AMICA), 52074, Aachen, Germany*
[4]*Institute for Theoretical Physics, TU Wien, 1040 Wien, Austria*
[5]*Research Center for Electronic and Optical Materials, National Institute for Materials Science, 1-1 Namiki, Tsukuba 305-0044, Japan*
[6]*Research Center for Materials Nanoarchitectonics, National Institute for Materials Science, 1-1 Namiki, Tsukuba 305-0044, Japan*
[7]*2nd Institute of Physics, University of Cologne, 50937 Köln, Germany*

(Received 25 February 2025; accepted 28 June 2025; published 19 August 2025)

We perform photoluminescence measurements on vacancy-related emitters in hexagonal boron nitride (hBN) that are notorious for their low quantum yields. The gating of these emitters via few-layer graphene electrodes reveals a reproducible, gate-dependent brightening of the emitter, which coincides with a change in the direction of the simultaneously measured leakage current across the hBN layers. At the same time, we observe that the relative increase of the brightening effect scales linearly with the intensity of the excitation laser. Both observations can be explained in terms of a photo-assisted electroluminescence effect. Interestingly, emitters can also show the opposite behavior, i.e., a decrease in emitter intensity that depends on the gate leakage current. We explain these two opposing behaviors by different concentrations of donor and acceptor states in the hBN and show that precise control of the doping of hBN is necessary to gain control over the brightness of vacancy-related emitters by electrical means. Our findings contribute to a deeper understanding of vacancy-related defect emitters in hBN that is necessary to make use of their potential in quantum information processing.

DOI: 10.1103/cd62-5hq8

Introduction. Hexagonal boron nitride (hBN) has emerged as a promising host material for quantum emitters [1–5]. Especially vacancy-related defects, e.g., defects consisting of a vacancy adjacent to a carbon substitutional, show significant potential for quantum information processing, as they can possess a triplet ground state and spin-conserving excited states [6–10]. In this respect, spin-lattice relaxation times of defect spins in the microsecond range [11,12] and room-temperature optical initialization and readout of triplet defect states have already been demonstrated [13]. However, whereas multi-carbon substitutional defects (e.g., carbon dimers and trimers) [14–16], can result in emitters exhibiting high brightness even at room temperature [17–22], vacancy-related defects are notorious for their low quantum yields [10,23]. In fact, the low brightness of vacancy-related defects has so far prevented second-order correlation ($g^{(2)}$) measurements and thus the unambiguous confirmation of their single photon emission [10]. Therefore, methods for the brightening of such dark emitters are of high interest. An effective method for tuning the emission energies and intensities of bright emitters was established by the integration of hBN into van der Waals heterostructures, which allow the use of optically transparent few-layer graphene gates [24–26]. This enables the precise control of the local electric field by applying voltages to the gates while maintaining optical access to the emitters. The reported variations in emitter intensity in response to the applied electric field have been attributed to several mechanisms, such as gate-induced (dis)charging of the emitter's charge-transition levels or of nearby defects [24–26]. These findings highlight the complex interplay between the local electronic environment and the optical properties of hBN emitters. A thorough understanding of this interplay might be crucial for paving the way towards quantum devices and sensors based on hBN emitters [5,10,22,27].

Here, we investigate the brightening of a dark hBN emitter that we assign to be a vacancy-carbon-substitutional (V-C) type defect by analyzing its phonon side bands (PSBs). Furthermore, we demonstrate that a gate-voltage-induced leakage current across the hBN layers appears to be responsible for the brightening effect. Our findings can be explained by a model that includes photo-assisted electroluminescence as the underlying mechanism of the reported intensity variations. Additionally, our results enable us to assign the different gate-dependent intensity variations observed in different emitters to differences in the doping

*Contact author: corinne.steiner@rwth-aachen.de
†Contact author: kurzmann@ph2.uni-koeln.de

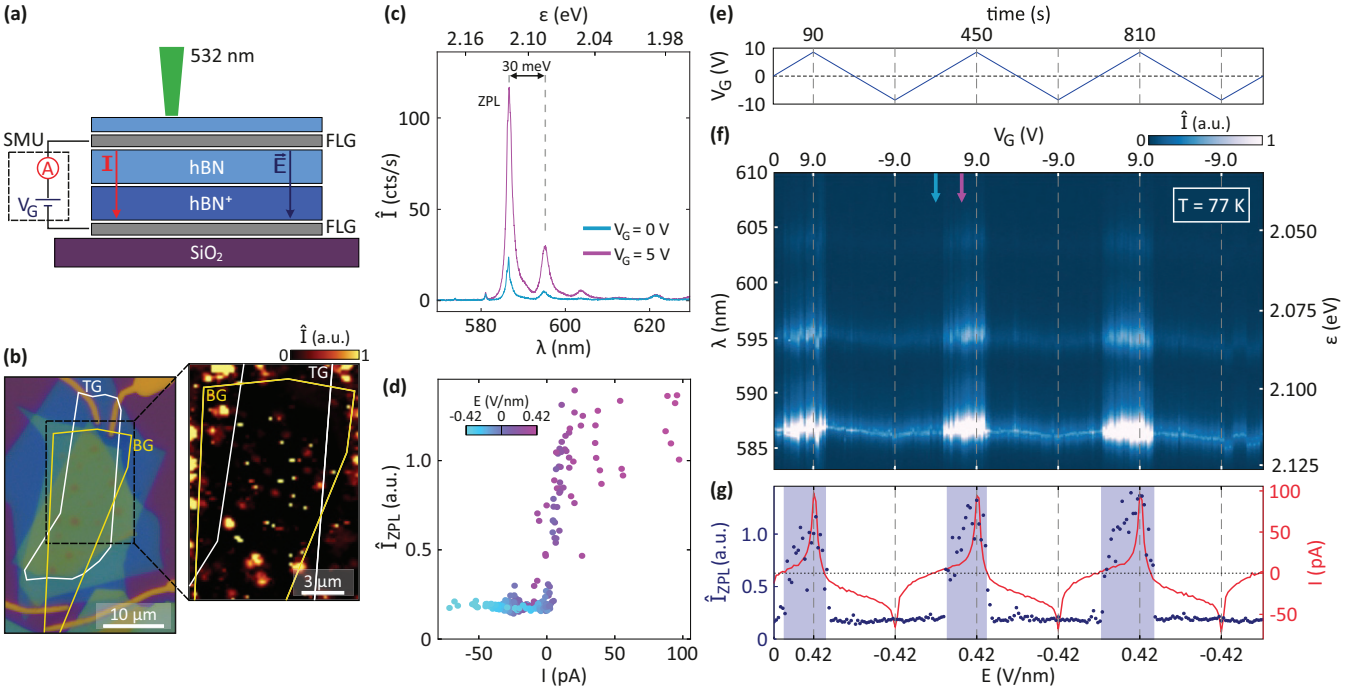

FIG. 1. (a) Schematic cross section of the few-layer graphene-gated hBN sample and its operating principle. The structure consists of an hBN emitter layer (hBN^+) and an hBN capping layer that are encapsulated in few-layer graphene (FLG) and stacked onto a Si/SiO_2 substrate. A source measurement unit (SMU) is used to apply a voltage (V_G) to the FLG gates and to simultaneously measure the leakage current I through the hBN. (b) Optical image of the sample. The outlines of the top and back gate are highlighted with white and yellow lines, respectively. (Zoom-in) Spatially resolved PL signal of the dual-gated area. Bright localized spots indicate the observable emitters in the hBN. (c) Comparison of a high intensity emitter spectrum at $V_G = 5$ V, corresponding to $E = 0.23$ V/nm, (magenta) and a low-intensity spectrum at $V_G = 0$ V (cyan). The ZPL and two additional side modes are visible and show gate-dependent intensity variations. Both spectra were measured at 77 K with a laser power of 200 µW. (d) The extracted zero phonon line (ZPL) intensity ($\hat{I}_{ZPL}$) of one emitter scales with the measured leakage current (color-coded to show its dependence on the applied external electric field E). (e) Illustration of how the gate voltage is swept in an alternating sequence over time between negative and positive values. (f) Corresponding PL spectra of the emitter during repeated gate voltage sweeps measured at $T = 77$ K and with a laser power of 200 µW. The emitter intensity is plotted as function of the applied gate voltage and electric field, respectively. The dashed gray lines mark the turning points of the voltage sweeps. The emitter shows a reproducible linear Stark shift and voltage-dependent changes in intensity. The blue and magenta arrows mark the spectra depicted in (c). (g) ZPL intensity obtained by taking the area of a Lorentzian function fitted to the ZPL peak from Fig. 1(f) (blue points). The blue shaded areas mark the electric field ranges where the emitter intensity is increased. The red curve shows the leakage current that was measured simultaneously to the PL signal. The dotted line indicates the zero-line of the current.

levels of the hBN. Therefore, our method of simultaneously measuring gate-dependent photoluminescence (PL) and gate leakage currents provides an additional and useful method for the characterization of both the hBN host material and its emitters.

Experimental methods. The structure of the graphene-gated hBN samples used for this Letter is shown schematically in Fig. 1(a). The samples consist of two hBN flakes that are encapsulated in few-layer graphene (FLG) flakes, resulting in a plate capacitor geometry. They were stacked and placed onto a Si^{++}/SiO_2 (285 nm) substrate using a dry transfer method [28–30]. Prior to the stacking, one hBN flake was thermally annealed (see the Supplemental Material [31] for process details) to induce emitters into the hBN flake [17] and is hereafter referred to as the emitter layer (hBN^+). The second hBN flake acts as a capping layer, separating the surface of the emitter layer from the FLG in order to prevent quenching of surface emitters caused by direct contact with graphene [32,33]. The FLG flakes serve as transparent, electrostatic gates, referred to as top gate (TG) and back gate (BG) and were contacted with lithographically defined Cr/Au contacts. Applying a gate voltage V_G between these two gates, i.e., electrodes, via a source measure unit [SMU, see Fig. 1(a)] allows us to study emitters in hBN under the influence of the induced out-of-plane electric field. Additionally, we can probe the voltage-induced leakage current that flows between the two electrodes through the hBN layers. Figure 1(b) shows an optical image of such a sample with yellow and white lines highlighting the outlines of the back and top gate, respectively. The zoom-in shown in the right panel of Fig. 1(b) depicts the spatially resolved photoluminescence signal of the black-marked area. Localized emission centers are visible as spatially confined bright yellow spots.

Results. We now focus on a specific emitter located within the dual-gated area of the sample, which exhibits a zero phonon line (ZPL) at approximately 587 nm (2.11 eV), see Fig. 1(c). The first thing to note is the very low brightness of the emitter of only up to around 120 counts per second at an excitation power of 200 µW and a laser spot size of about 500 nm. Such a low quantum yield is characteristic

of vacancy-related defects [10,23]. Further support for the assignment of the emitter as a vacancy-related defect comes from the examination of the phonon side bands (PSBs), which can be observed in PL measurements conducted at a temperature of 77 K (see the Supplemental Material [31] for 4 K data of the emitter). These PSBs are separated from the ZPL by an energy difference of around 30 meV, which is much lower than the typical energy separation of 160 ± 20 meV commonly observed for bright emitters [1,3,14,17,18,34,35]. This reduced energy separation corresponds well with defect breathing modes of vacancy-related defects in hBN [36,37]. Because of the large spectral weight of these breathing modes [38], vacancy-related defects are not expected to show pronounced PSBs in the normally observable energy range. Moreover, the specific positions of the PSBs in the spectrum shown in Fig. 1(c) are found to be in agreement with theoretical predictions for a vacancy-carbon substitutional defect [36,38] suggesting that our experimentally observed emitter is indeed hosted by a V-C defect type (for further discussion, see the Supplemental Material [31]).

Next, we focus on the gate voltage dependence of the emission properties of this dark emitter. As seen in Fig. 1(c), the intensity of the emitter varies significantly between the two depicted spectra recorded at $V_G = 0$ V and $V_G = 5$ V. To investigate the brightening effect in more detail, we sweep the applied gate voltage V_G in repeated cycles between –9 V and 9 V, as illustrated in Fig. 1(e). During these cycles, we simultaneously measure the leakage current flowing through the FLG/hBN/FLG structure and record PL spectra of the emitter. The color-coded plot in Fig. 1(f) shows these spectra as a function of the resulting electrical field, which was calculated from the applied gate voltage according to the Lorentz local field approximation [24,39] [$E = ((\epsilon_{hBN} + 2) \times V_G)/(3t)$, with the permittivity $\epsilon_{hBN} = 3.4$ and the combined thickness $t = 39$ nm of both hBN layers]. Over the repeated sweep cycles of the gate voltage we observe a linear Stark shift of 0.54 ± 0.04 nm/(V/nm) and notably a clear and reproducible brightening of the emitter's ZPL and PSBs. This linear Stark shift is consistent with an emitter exhibiting a permanent electric dipole moment, a consequence of the defect's geometry breaking the inversion symmetry with respect to the hBN lattice plane [24,40–42].

During the upward sweeps of the gate voltage, the emitter intensity increases abruptly before returning to its original intensity during the sweep back down to zero gate voltage. This is exemplary shown in Fig. 1(c), which depicts two spectra at $V_G = 0$ V and $V_G = 5$ V that correspond to line cuts in Fig. 1(f) (see blue and magenta arrows). A direct comparison of the peak intensities, which were obtained by fitting a Lorentzian curve to the measured spectra, reveals that the intensity increases by up to a factor of six. It is noteworthy that this increase only happens at positive gate voltages. Within the voltage range from $V_G = 0$ V to –9 V no increase in intensity is observed. Furthermore, by comparing the gate voltage values where the emitter switches its intensity from dark to bright with the values where the intensity switches back to its darker state it is apparent that the intensity variations follow a hysteretic behavior (see the Supplemental Material [31] for further discussion). In order to explore the interplay of the observed intensity variations with the leakage

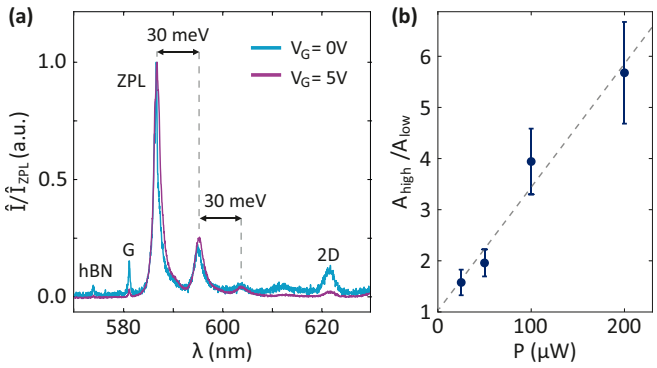

FIG. 2. (a) Comparison of the two spectra shown in Fig. 1(c) with their intensity normalized to 1. For the sake of clarity, peaks related to the Raman signals of hBN (574 nm [43]) and graphene (G peak at 581 nm and 2D peak at 620 nm [44]), which do not scale have been labeled. (b) Ratio between the bright and dark ZPL amplitudes as a function of the power of the excitation laser (laser spot size of around 500 nm). The dashed gray line serves as a guide to the eye and depicts ideal linear behavior.

current through the hBN, the extracted peak intensities of the ZPL (blue points) are plotted alongside the simultaneously measured current (red curve) in Fig. 1(g). This comparison reveals that the intensity variations of the emitter are directly linked to the current I through the hBN. Specifically, the transitions from negative to positive current directions (see the intersections between the red curve and the gray dashed line, the latter depicting the $I = 0$ pA level) coincide closely with the emitter switching between its dark and bright state. This observation becomes even more evident when the ZPL intensity is plotted as a function of the leakage current, as depicted in Fig. 1(d). A distinct transition from low to high ZPL intensity is observed around zero leakage current, emphasizing the role of the current in modulating the brightness of the emitter. Note that the measured leakage current consists of multiple contributions, leading to a nonperfect coincidence between the direction change of the measured current and the intensity increase (see the Supplemental Material [31]). We note that, except for the shift in wavelength caused by the Stark effect, the ZPLs as well as the PSBs match each other for both the dark and the bright states, as is evident when comparing spectra of the emitter with the ZPL normalized to 1 as shown in Fig. 2(a). Furthermore, we identify that a laser-induced photoexcitation process must play a crucial role in the brightening effect of the emitter distinguishing it from a pure electroluminescence effect [45,46]. For this, Fig. 2(b) shows the ratio of the ZPL amplitudes in the bright and dark states as a function of laser excitation power, which reveals that the brightening effect becomes increasingly pronounced at higher laser powers. We are not aware of any electrostatic (dis)charging effects, which were previously attributed to intensity variations of bright hBN emitters [24–26], that would depend on laser power in such a manner. Moreover, the features of the observed brightening are not consistent with an intensity modulation induced by a quantum confined Stark effect (QCSE), as the latter is expected to be continuous in electric field and not dependent on the excitation power [41,47] (see the Supplemental Material [31] for detailed

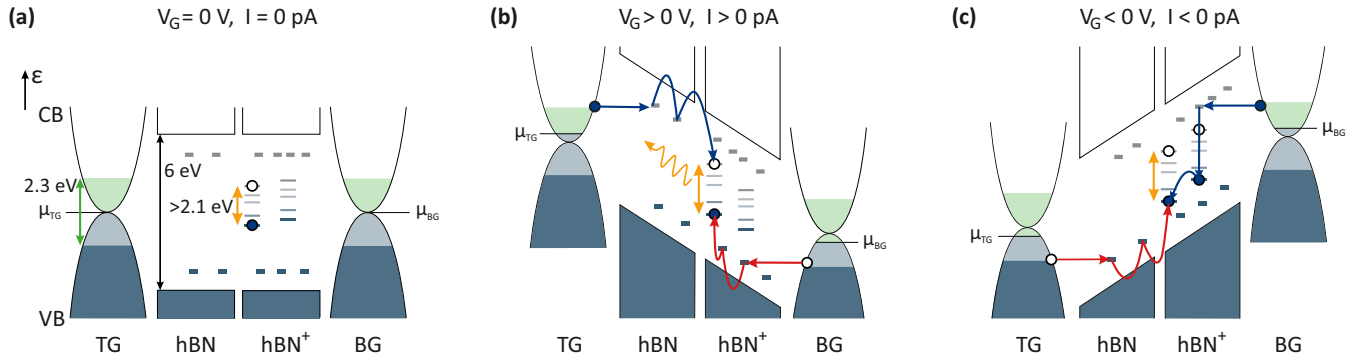

FIG. 3. Model that links changes in the charge transport across the hBN layers to the intensity variations of the emitter in the hBN^+ layer. The top gate (TG) and the bottom gate (BG) are made of few-layer graphene. (a) At $V_G = 0$ V, no charge transport through the hBN occurs and the emitter can only be excited by optical absorption in the hBN^+ layer. (b) For $V_G > 0$, photoexcited electrons (filled circles) and holes (open circles) from the gate electrodes, (shaded areas in the band structure of the FLG), undergo a photo-assisted field emission into carbon-related donor and acceptor states, depicted by blue and red arrows, respectively. Electrons and holes flow towards the emitter in the hBN^+ via laser-induced Poole-Frenkel like emission (blue and red curved lines) and recombine over the energy levels of the emitter, creating the brightening effect caused by electroluminescence. (c) For $V_G < 0$, electrons injected by the back gate electrode scatter into mid-gap states of the emitter layer before reaching the emitter, suppressing the electroluminescence effect.

discussion). It can thus be concluded that the brightening of the dark emitter necessitates a photoexcitation process that is also closely linked to the leakage current across the hBN layers, as shown in Fig. 1(d).

Based on the above arguments, we present a model (see Fig. 3) that proposes a photo-assisted injection of charge carriers— driven by the interplay of laser excitation and gate voltage—as the mechanism responsible for the brightening of the emitter.

We approximate the gapless band structure of the FLG top and bottom gates (TG and BG) by two parabolic bands [48]. At zero gate voltage, the respective chemical potentials $\mu_{TG,BG}$ of the two gates are positioned at the charge neutrality points [Fig. 3(a)]. Under laser illumination ($\varepsilon = 2.3$ eV), electrons in the gate electrodes are excited from the valence into the conduction band [indicated by the blue and green shaded areas in Fig. 3(a)], creating photoexcited electrons and holes up to 1.15 eV away from the chemical potentials. We note that scattering processes among these photoexcited charge carriers may push a small fraction of them to even higher energy states [49–51]. We now discuss the mechanism by which charge carriers can be injected from the FLG electrodes into the hBN layers. First, we note that the electric field strength at which the leakage current across the hBN begins to show a strongly nonlinear increase in Fig. 1(g) is rather small in comparison to reference samples that are not showing a current-induced brightening effect (see the Supplemental Material [31]). We attribute this low threshold voltage to the onset of photo-assisted field emission [52,53] into carbon monomer defect (C_B, C_N) states present in the hBN [54,55] (see the Supplemental Material [31] for detailed discussion). These defects can form both donor and acceptor states based on whether the carbon atom replaces a boron (C_B) or a nitrogen atom (C_N) [56–61], as illustrated by the discrete energy states (grey and blue short dashes) in the hBN band gap in Fig. 3. Depending on the calculation method [62], the corresponding energy states are predicted to lie anywhere from a few hundred meV up to 1.5 eV below the conduction band or above the valence band edge [56–61]. Furthermore, carbon monomers have been proposed to conduct gate leakage currents across the hBN layers [54,55]. We therefore assume that under the application of a gate voltage [see Fig. 3(b)], photoexcited charge carriers from the gate electrodes undergo photo-assisted field emission [52,53] into these carbon monomer states [depicted by the horizontal, blue, and red arrows in Fig. 3(b)]. The rate of such a photo-assisted field emission is expected to depend nonlinearly on the electric field strength and linearly on the laser intensity, as described by Fowler-Nordheim theory [52,53]. The predicted nonlinear dependence on the electric field is observed in the current plotted in Fig. 1(g) at higher gate voltages. The predicted linear dependence on the laser intensity is consistent with the laser power dependence shown in Fig. 2(b) (see also a previous study from some of us in Ref. [63]), supporting that the brightening effect is indeed caused by a photo-assisted electroluminescence effect. Because of the continuous laser illumination, charge carriers get continuously injected into the defect donor and acceptor states, allowing them to follow the externally applied gate electric field by hopping between different defect states via Poole-Frenkel like emission [64] (represented by the curved blue and red lines for donor and acceptor states, respectively; full circles represent electrons, hollow ones holes). Note that this excitation mechanism and the corresponding photo-induced transport of charges between hBN and adjacent two-dimensional materials are in accordance with studies on photo-doping effects in van der Waals heterostructures using hBN as a dielectric layer [65–69]. The injection of both electrons into the hBN from one gate electrode and holes into the hBN^+ from the other electrode [see Fig. 3(b)] leads to an explanation for the observed brightening of the emitter's ZPL and its connection to the leakage current across the hBN. The brightening effect can be understood in terms of photoexcited electron-hole pairs that recombine over the energy levels of the emitter and thus create additional electroluminescence—an effect that

we denote as photo-assisted electroluminescence [see orange curved arrow in Fig. 3(b)]. We support this proposed mechanism by theoretical simulations that can be found in the Supplemental Material [31].

Next, we focus on the asymmetry of the brightening effect with respect to the gate voltage polarity and the resulting induced leakage current. As we will explain in the following, this asymmetry is a direct consequence of the asymmetry in the sample structure and can be described by theoretical simulations using a rate equation model (see the Supplemental Material [31]). Because of the emitter generation process by annealing, it is likely that additional vacancy complexes (e.g., multivacancy or vacancy-substitutional defects) have been created in the hBN^+ that are not present in the untreated hBN layer. These defects may lack radiative recombination channels or be quenched because of their proximity to the FLG electrode [32,33] but they provide extra energy states within the hBN^+. Importantly, in contrast to carbon monomer defects present in both hBN layers—which create single donor or acceptor energy states—vacancy complexes can exhibit energy levels with a series of occupied and unoccupied states extending over the entire band gap range at the location of the defect (see the thin-stacked lines spanning over the hBN^+ band gap in Fig. 3 and the more detailed discussion in the Supplemental Material [31]) [6,7,38,56–59,70,70–73]. With this, the observed gate voltage asymmetry can now be explained under the assumption that the energy levels of these vacancy complexes that are only present in the hBN^+ may allow for additional charge relaxation channels with differing relaxation rates for electrons and holes. At negative gate voltages, holes from the TG are injected into the hBN layer and can reach the emitter in the hBN^+ by hopping between acceptor states (as for the positive gate voltage case). However, electrons injected from the BG now have additional relaxation channels within the hBN^+, making it less likely that they will reach the upper emitter level related to the optical emission. Figure 3(c) provides a simplified illustration of this process by showing that holes do not relax before reaching the emitter while electrons do [compare red lines in Fig. 3(b) with the blue lines in Fig. 3(c)]. In fact, as we discuss in the Supplemental Material [31], it is sufficient that only a fraction of holes does not relax before reaching the emitter. Provided that the relaxation of excited electrons into mid-gap states effectively prevents the occupation of the upper energy level of the emitter, the electroluminescence effect can be captured adequately by the presented model.

Interestingly, we also find hBN emitters that do not exhibit a brightening but rather show a current (gate-voltage) induced *de*crease in their emission intensity. Such an emitter is presented in Fig. 4. The emitter is located in a second sample with the same stacking order as shown in Fig. 1(a). Both the position of the ZPL at 590.7 nm and the strength of the linear Stark shift of $s = 0.73 \pm 0.01\,\mathrm{nm/(V/nm)}$ are similar to the other emitter [compare Fig. 1(f) with Fig. 4(a)]. However, at positive electric field values, the emitter intensity now decreases in contrast to the previously discussed increase in intensity. Analogous to the first emitter, the change in intensity [blue data points in Fig. 4(b)] coincides with the direction of the leakage current switching from negative to positive values [red line in Fig. 4(b)] [74].

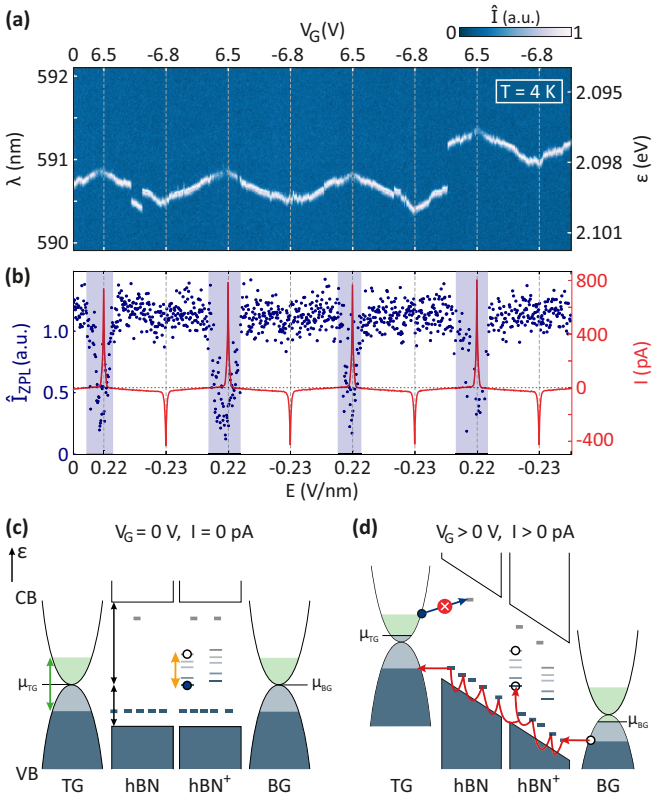

FIG. 4. Gate voltage dependence of emitter intensity and leakage current of a second emitter in a different sample with a ZPL at 590.7 nm measured at 4 K with a laser power of 50 μW. (a) Emitter intensity as a function of the applied electric field. The emitter exhibits a reproducible linear Stark shift and voltage-dependent changes in intensity. (b) Integrated ZPL intensity of Lorentz fitted peaks from (a). The red curve depicts the simultaneously measured gate leakage current. The blue shaded areas mark the electric field ranges where the emitter intensity is decreased. As for the first emitter, a clear dependence of the intensity change on the gate leakage current is observed. (c), (d) Adapted schematic of the previously discussed model for this emitter. All notations like in Fig. 3. Panel (c) depicts the case for $V_G = 0$. The chemical potentials of the FLG electrodes are shifted towards the hBN valence band corresponding to the case of p-doped hBN. (d) For $V_G > 0$ electron injection and thus electron-hole recombination in the emitter levels is blocked. Occasional de-occupation of the lower emitter layer blocks its PL emission.

We now demonstrate that our model allows us to understand this darkening effect by assuming different doping in the hBN layers of the two samples. For the first emitter, we assumed a rough balance of donor and acceptor states (Fig. 3), which resulted in the chemical potentials of the FLG electrodes being aligned approximately to the center of the band gap of the hBN layers. Such an alignment can indeed be observed in several angle-resolved photoemission spectroscopy (ARPES) or scanning tunneling spectroscopy (STS) studies [57,71,75]. For the second emitter, we now assume p-doped hBN for which other studies have shown a pronounced shift of the chemical potentials towards the valence band of the hBN [76–78] [see Fig. 4(c) for $V_G = 0$]. This p-doping requires an excess of acceptor states near the valence band edge that leads to a shift in the band alignment of the hBN

relative to the FLG electrodes, where the chemical potentials of the electrodes are now no longer in the center of the hBN band gap, but shifted closer to the hBN valence band edge. As a result, the dielectric strength of a structure with such a band alignment would be reduced as it is indeed observed for the second sample (see the Supplemental Material [31]). Based on this change in band alignment, the darkening of the emitter can now be understood from Fig. 4(d). Here, the band alignment corresponds to p-doped hBN and is depicted for a positive gate voltage $V_G > 0$, for which this emitter shows a decrease in intensity [in contrast to the brightening effect, compare Fig. 1(f) and Fig. 3(b)]. Because of the shift of the chemical potential towards the valence band, the top gate can no longer inject electrons into donor states of the hBN capping layer [see red cross symbol in Fig. 4(d)]. Instead, the whole leakage current over the hBN is carried via holes over states near the valence band edge (see curved red arrows). The lack of electron injection inhibits electron-hole pair recombination via the energy levels of the emitter, i.e., there is no photo-assisted electroluminescence effect. Instead, the lower level of the emitter occasionally becomes unoccupied because of holes that enter the lower emitter level, visualized in Fig. 4(d). These holes have a long residence time within this level because of the potential barrier formed by the low defect density capping layer. During such times, the emitter can no longer be optically excited, leading to an effective decrease in emitter intensity. For negative voltages, holes may still enter the lower emitter level but are not stuck there because the defect density within the emitter layer provides only small potential barriers towards the next energy level. Thus, the photoluminescence of the emitter is not blocked and the intensity does not change (see the Supplemental Material [31] for detailed analysis of the $V_G < 0$ case).

Conclusions. In summary, we have demonstrated that the intensity of V-C type hBN emitters can be modulated by photo-assisted electroluminescence. For this, the necessary leakage current is injected into the hBN layers from few-layer graphene gates via photo-assisted field emission. Depending on the doping level of the hBN layers, we propose that the leakage current can either consist of both electrons and holes or only of holes. The first case leads to the possibility of electron-hole pairs recombining at the location of the emitter, resulting in its brightening, whereas the second case results in the sporadic de-occupation of the emitter's lower energy level, resulting in the emitter getting even darker. Our findings highlight the necessity for a reliable benchmarking of hBN crystals [79,80] and the need for a careful determination of their doping levels in order to achieve electronic control over the brightness of dark quantum emitters in hBN.

Acknowledgments. The authors thank F. Lentz and S. Trellenkamp for their support in sample fabrication. Funded by the Deutsche Forschungsgemeinschaft (DFG, German Research Foundation) under Germany's Excellence Strategy - Cluster of Excellence Matter and Light for Quantum Computing (ML4Q) EXC 2004/1 - 390534769 and by the Federal Ministry of Education and Research (BMBF) and the Ministry of Culture and Science of the German State of North Rhine-Westphalia (MKW) under the Excellence Strategy of the Federal Government and the Länder. K.W. and T.T. acknowledge support from the JSPS KAKENHI (Grants No. 21H05233 and No. 23H02052) and World Premier International Research Center Initiative (WPI), MEXT, Japan. This research was funded in part by the Austrian Science Fund (FWF) [10.55776/DOC142, 10.55776/COE5]. Fabrication of the samples was supported by the Helmholtz Nano Facility (HNF) at the Forschungszentrum Jülich [98].

The authors declare no competing interests.

Data availability. The data supporting the findings of this study are openly available [99].

[1] T. T. Tran, K. Bray, M. J. Ford, M. Toth, and I. Aharonovich, Quantum emission from hexagonal boron nitride monolayers, Nat. Nanotechnol. **11**, 37 (2016).

[2] T. T. Tran, C. Zachreson, A. M. Berhane, K. Bray, R. G. Sandstrom, L. H. Li, T. Taniguchi, K. Watanabe, I. Aharonovich, and M. Toth, Quantum emission from defects in single-crystalline hexagonal boron nitride, Phys. Rev. Appl. **5**, 034005 (2016).

[3] L. J. Martínez, T. Pelini, V. Waselowski, J. R. Maze, B. Gil, G. Cassabois, and V. Jacques, Efficient single photon emission from a high-purity hexagonal boron nitride crystal, Phys. Rev. B **94**, 121405 (2016).

[4] S. Choi, T. T. Tran, C. Elbadawi, C. Lobo, X. Wang, S. Juodkazis, G. Seniutinas, M. Toth, and I. Aharonovich, Engineering and localization of quantum emitters in large hexagonal boron nitride layers, ACS Appl. Mater. Interfaces **8**, 29642 (2016).

[5] J. D. Caldwell, I. Aharonovich, G. Cassabois, J. H. Edgar, B. Gil, and D. N. Basov, Photonics with hexagonal boron nitride, Nat. Rev. Mater. **4**, 552 (2019).

[6] F. Wu, A. Galatas, R. Sundararaman, D. Rocca, and Y. Ping, First-principles engineering of charged defects for two-dimensional quantum technologies, Phys. Rev. Mater. **1**, 071001 (2017).

[7] A. Sajid, J. R. Reimers, and M. J. Ford, Defect states in hexagonal boron nitride: Assignments of observed properties and prediction of properties relevant to quantum computation, Phys. Rev. B **97**, 064101 (2018).

[8] G. Cheng, Y. Zhang, L. Yan, H. Huang, Q. Huang, Y. Song, Y. Chen, and Z. Tang, A paramagnetic neutral C_BV_N center in hexagonal boron nitride monolayer for spin qubit application, Comput. Mater. Sci. **129**, 247 (2017).

[9] V. Ivády, G. Barcza, G. Thiering, S. Li, H. Hamdi, J.-P. Chou, O. Legeza, and A. Gali, *Ab initio* theory of the negatively charged boron vacancy qubit in hexagonal boron nitride, npj Comput. Mater. **6**, 41 (2020).

[10] S. Vaidya, X. Gao, S. Dikshit, I. Aharonovich, and T. Li, Quantum sensing and imaging with spin defects in hexagonal boron nitride, Adv. Phys.: X **8**, 2206049 (2023).

[11] A. Gottscholl, M. Diez, V. Soltamov, C. Kasper, A. Sperlich, M. Kianinia, C. Bradac, I. Aharonovich, and V. Dyakonov, Room temperature coherent control of spin defects in hexagonal boron nitride, Sci. Adv. **7**, eabf3630 (2021).

[12] N. Chejanovsky, A. Mukherjee, J. Geng, Y.-C. Chen, Y. Kim, A. Denisenko, A. Finkler, T. Taniguchi, K. Watanabe, D. B. R. Dasari *et al.*, Single-spin resonance in a van der Waals embedded paramagnetic defect, Nat. Mater. **20**, 1079 (2021).

[13] A. Gottscholl, M. Kianinia, V. Soltamov, S. Orlinskii, G. Mamin, C. Bradac, C. Kasper, K. Krambrock, A. Sperlich, M. Toth *et al.*, Initialization and read-out of intrinsic spin defects in a van der Waals crystal at room temperature, Nat. Mater. **19**, 540 (2020).

[14] N. Mendelson, D. Chugh, J. R. Reimers, T. S. Cheng, A. Gottscholl, H. Long, C. J. Mellor, A. Zettl, V. Dyakonov, P. H. Beton *et al.*, Identifying carbon as the source of visible single-photon emission from hexagonal boron nitride, Nat. Mater. **20**, 321 (2021).

[15] K. Li, T. J. Smart, and Y. Ping, Carbon trimer as a 2 eV single-photon emitter candidate in hexagonal boron nitride: A first-principles study, Phys. Rev. Mater. **6**, L042201 (2022).

[16] A. Kumar, C. Cholsuk, A. Zand, M. N. Mishuk, T. Matthes, F. Eilenberger, S. Suwanna, and T. Vogl, Localized creation of yellow single photon emitting carbon complexes in hexagonal boron nitride, APL Mater. **11**, 071108 (2023).

[17] T. T. Tran, C. Elbadawi, D. Totonjian, C. J. Lobo, G. Grosso, H. Moon, D. R. Englund, M. J. Ford, I. Aharonovich, and M. Toth, Robust multicolor single photon emission from point defects in hexagonal boron nitride, ACS Nano **10**, 7331 (2016).

[18] N. Chejanovsky, M. Rezai, F. Paolucci, Y. Kim, T. Rendler, W. Rouabeh, F. Fávaro de Oliveira, P. Herlinger, A. Denisenko, S. Yang *et al.*, Structural attributes and photodynamics of visible spectrum quantum emitters in hexagonal boron nitride, Nano Lett. **16**, 7037 (2016).

[19] G. Grosso, H. Moon, B. Lienhard, S. Ali, D. K. Efetov, M. M. Furchi, P. Jarillo-Herrero, M. J. Ford, I. Aharonovich, and D. Englund, Tunable and high-purity room temperature single-photon emission from atomic defects in hexagonal boron nitride, Nat. Commun. **8**, 705 (2017).

[20] N. R. Jungwirth, B. Calderon, Y. Ji, M. G. Spencer, M. E. Flatté, and G. D. Fuchs, Temperature dependence of wavelength selectable zero-phonon emission from single defects in hexagonal boron nitride, Nano Lett. **16**, 6052 (2016).

[21] N. V. Proscia, Z. Shotan, H. Jayakumar, P. Reddy, C. Cohen, M. Dollar, A. Alkauskas, M. Doherty, C. A. Meriles, and V. M. Menon, Near-deterministic activation of room-temperature quantum emitters in hexagonal boron nitride, Optica **5**, 1128 (2018).

[22] I. Aharonovich, J.-P. Tetienne, and M. Toth, Quantum emitters in hexagonal boron nitride, Nano Lett. **22**, 9227 (2022).

[23] J. R. Reimers, J. Shen, M. Kianinia, C. Bradac, I. Aharonovich, M. J. Ford, and P. Piecuch, Photoluminescence, photophysics, and photochemistry of the V_B^- defect in hexagonal boron nitride, Phys. Rev. B **102**, 144105 (2020).

[24] G. Noh, D. Choi, J.-H. Kim, D.-G. Im, Y.-H. Kim, H. Seo, and J. Lee, Stark tuning of single-photon emitters in hexagonal boron nitride, Nano Lett. **18**, 4710 (2018).

[25] M. Yu, D. Yim, H. Seo, and J. Lee, Electrical charge control of h-BN single photon sources, 2D Mater. **9**, 035020 (2022).

[26] S. J. U. White, T. Yang, N. Dontschuk, C. Li, Z.-Q. Xu, M. Kianinia, A. Stacey, M. Toth, and I. Aharonovich, Electrical control of quantum emitters in a van der Waals heterostructure, Light Sci. Appl. **11**, 186 (2022).

[27] H.-H. Fang, X.-J. Wang, X. Marie, and H.-B. Sun, Quantum sensing with optically accessible spin defects in van der Waals layered materials, Light Sci. Appl. **13**, 303 (2024).

[28] F. Pizzocchero, L. Gammelgaard, B. S. Jessen, J. M. Caridad, L. Wang, J. Hone, P. Bøggild, and T. J. Booth, The hot pick-up technique for batch assembly of van der Waals heterostructures, Nat. Commun. **7**, 11894 (2016).

[29] L. Banszerus, H. Janssen, M. Otto, A. Epping, T. Taniguchi, K. Watanabe, B. Beschoten, D. Neumaier, and C. Stampfer, Identifying suitable substrates for high-quality graphene-based heterostructures, 2D Mater. **4**, 025030 (2017).

[30] T. Bisswanger, Z. Winter, A. Schmidt, F. Volmer, K. Watanabe, T. Taniguchi, C. Stampfer, and B. Beschoten, CVD bilayer graphene spin valves with 26 μm spin diffusion length at room temperature, Nano Lett. **22**, 4949 (2022).

[31] See Supplemental Material at http://link.aps.org/supplemental/10.1103/cd62-5hq8 for (1) details on sample fabrication, (2) details on the measurement setup, (3) measurements of emitter 1 at 4K, (4) an analysis of the negative voltage case for the darkening emitter, (5) discussion on the magnitude of leakage current vs increase in brightness of the emitter, (6) a discussion on the contributions to leakage current, (7) a discussion on the physical origin of the leakage current, (8) a discussion on the electron-hole asymmetry, (9) a discussion on the hysteresis effect of the gate-dependent brightening effect, (10) discussion on brightening effects in emitters owing to the QCSE, and (11) theoretical simulations of the charge distribution and relaxation processes, which also includes Refs. [[6,8,14,38,41,47,52–61,63,65–69,72,81–97]].

[32] J. C. Stewart, Y. Fan, J. S. H. Danial, A. Goetz, A. S. Prasad, O. J. Burton, J. A. Alexander-Webber, S. F. Lee, S. M. Skoff, V. Babenko, and S. Hofmann, Quantum emitter localization in layer-engineered hexagonal boron nitride, ACS Nano **15**, 13591 (2021).

[33] D. Tebbe, M. Schütte, K. Watanabe, T. Taniguchi, C. Stampfer, B. Beschoten, and L. Waldecker, Distance dependence of the energy transfer mechanism in WS_2-graphene heterostructures, Phys. Rev. Lett. **132**, 196902 (2024).

[34] C. Fournier, A. Plaud, S. Roux, A. Pierret, M. Rosticher, K. Watanabe, T. Taniguchi, S. Buil, X. Quélin, J. Barjon *et al.*, Position-controlled quantum emitters with reproducible emission wavelength in hexagonal boron nitride, Nat. Commun. **12**, 3779 (2021).

[35] F. Hayee, L. Yu, J. L. Zhang, C. J. Ciccarino, M. Nguyen, A. F. Marshall, I. Aharonovich, J. Vučković, P. Narang, T. F. Heinz, and J. A. Dionne, Revealing multiple classes of stable quantum emitters in hexagonal boron nitride with correlated optical and electron microscopy, Nat. Mater. **19**, 534 (2020).

[36] S. A. Tawfik, S. Ali, M. Fronzi, M. Kianinia, T. T. Tran, C. Stampfl, I. Aharonovich, M. Toth, and M. J. Ford, First-principles investigation of quantum emission from hBN defects, Nanoscale **9**, 13575 (2017).

[37] G. Grosso, H. Moon, C. J. Ciccarino, J. Flick, N. Mendelson, L. Mennel, M. Toth, I. Aharonovich, P. Narang, and D. R. Englund, Low-temperature electron–phonon interaction of quantum emitters in hexagonal boron nitride, ACS Photon. **7**, 1410 (2020).

[38] C. Jara, T. Rauch, S. Botti, M. A. L. Marques, A. Norambuena, R. Coto, J. E. Castellanos-águila, J. R. Maze, and F. Munoz,

First-principles identification of single photon emitters based on carbon clusters in hexagonal boron nitride, J. Phys. Chem. A **125**, 1325 (2021).

[39] A. Scavuzzo, S. Mangel, J.-H. Park, S. Lee, D. Loc Duong, C. Strelow, A. Mews, M. Burghard, and K. Kern, Electrically tunable quantum emitters in an ultrathin graphene–hexagonal boron nitride van der Waals heterostructure, Appl. Phys. Lett. **114**, 062104 (2019).

[40] J. G. Roch, N. Leisgang, G. Froehlicher, P. Makk, K. Watanabe, T. Taniguchi, C. Schönenberger, and R. J. Warburton, Quantum-confined stark effect in a MoS_2 monolayer van der Waals heterostructure, Nano Lett. **18**, 1070 (2018).

[41] Y. Xia, Q. Li, J. Kim, W. Bao, C. Gong, S. Yang, Y. Wang, and X. Zhang, Room-temperature giant Stark effect of single photon emitter in van der Waals material, Nano Lett. **19**, 7100 (2019).

[42] L. Linhart, M. Paur, V. Smejkal, J. Burgdörfer, T. Mueller, and F. Libisch, Localized intervalley defect excitons as single-photon emitters in WSe_2, Phys. Rev. Lett. **123**, 146401 (2019).

[43] X. Li, J. Liu, K. Ding, X. Zhao, S. Li, W. Zhou, and B. Liang, Temperature dependence of Raman-active in-plane E_2g phonons in layered graphene and h-BN flakes, Nanoscale Res. Lett. **13**, 25 (2018).

[44] A. C. Ferrari, J. C. Meyer, V. Scardaci, C. Casiraghi, M. Lazzeri, F. Mauri, S. Piscanec, D. Jiang, K. S. Novoselov, S. Roth, and A. K. Geim, Raman spectrum of graphene and graphene layers, Phys. Rev. Lett. **97**, 187401 (2006).

[45] G. Park, I. Zhigulin, H. Jung, J. Horder, K. Yamamura, Y. Han, H. Cho, H.-W. Jeong, K. Watanabe, T. Taniguchi *et al.*, Narrowband electroluminescence from color centers in hexagonal boron nitride, Nano Lett. **24**, 15268 (2024).

[46] M. Yu, J. Lee, K. Watanabe, T. Taniguchi, and J. Lee, Electrically pumped h-BN single-photon emission in van der Waals heterostructure, ACS Nano **19**, 504 (2025).

[47] C. Chakraborty, K. M. Goodfellow, S. Dhara, A. Yoshimura, V. Meunier, and A. N. Vamivakas, Quantum-confined stark effect of individual defects in a van der Waals heterostructure, Nano Lett. **17**, 2253 (2017).

[48] K. F. Mak, J. Shan, and T. F. Heinz, Electronic structure of few-layer graphene: Experimental demonstration of strong dependence on stacking sequence, Phys. Rev. Lett. **104**, 176404 (2010).

[49] T. Li, L. Luo, M. Hupalo, J. Zhang, M. C. Tringides, J. Schmalian, and J. Wang, Femtosecond population inversion and stimulated emission of dense Dirac fermions in graphene, Phys. Rev. Lett. **108**, 167401 (2012).

[50] D. Brida, A. Tomadin, C. Manzoni, Y. J. Kim, A. Lombardo, S. Milana, R. R. Nair, K. S. Novoselov, A. C. Ferrari, G. Cerullo, and M. Polini, Ultrafast collinear scattering and carrier multiplication in graphene, Nat. Commun. **4**, 1987 (2013).

[51] Y. Chen, Y. Li, Y. Zhao, H. Zhou, and H. Zhu, Highly efficient hot electron harvesting from graphene before electron-hole thermalization, Sci. Adv. **5**, eaax9958 (2019).

[52] R. Haindl, K. Köster, J. H. Gaida, M. Franz, A. Feist, and C. Ropers, Femtosecond tunable-wavelength photoassisted cold field emission, Appl. Phys. B **129**, 40 (2023).

[53] M. Krüger, C. Lemell, G. Wachter, J. Burgdörfer, and P. Hommelhoff, Attosecond physics phenomena at nanometric tips, J. Phys. B: At. Mol. Opt. Phys. **51**, 172001 (2018).

[54] Z. Huang, R.-G. Lee, E. Cuniberto, J. Song, J. Lee, A. Alharbi, K. Kisslinger, T. Taniguchi, K. Watanabe, Y.-H. Kim, and D. Shahrjerdi, Characterizing defects inside hexagonal boron nitride using random telegraph signals in van der Waals 2D transistors, ACS Nano **18**, 28700 (2024).

[55] U. Chandni, K. Watanabe, T. Taniguchi, and J. P. Eisenstein, Evidence for defect-mediated tunneling in hexagonal boron nitride-based junctions, Nano Lett. **15**, 7329 (2015).

[56] D. I. Badrtdinov, C. Rodriguez-Fernandez, M. Grzeszczyk, Z. Qiu, K. Vaklinova, P. Huang, A. Hampel, K. Watanabe, T. Taniguchi, L. Jiong *et al.*, Dielectric environment sensitivity of carbon centers in hexagonal boron nitride, Small **19**, 2300144 (2023).

[57] R. J. P. Román, F. J. R. C. Costa, A. Zobelli, C. Elias, P. Valvin, G. Cassabois, B. Gil, A. Summerfield, T. S. Cheng, C. J. Mellor *et al.*, Band gap measurements of monolayer h-BN and insights into carbon-related point defects, 2D Mater. **8**, 044001 (2021).

[58] P. Huang, M. Grzeszczyk, K. Vaklinova, K. Watanabe, T. Taniguchi, K. S. Novoselov, and M. Koperski, Carbon and vacancy centers in hexagonal boron nitride, Phys. Rev. B **106**, 014107 (2022).

[59] C. Su, F. Zhang, S. Kahn, B. Shevitski, J. Jiang, C. Dai, A. Ungar, J.-H. Park, K. Watanabe, T. Taniguchi *et al.*, Tuning colour centres at a twisted hexagonal boron nitride interface, Nat. Mater. **21**, 896 (2022).

[60] M. Mackoit-Sinkevičienė, M. Maciaszek, C. G. Van de Walle, and A. Alkauskas, Carbon dimer defect as a source of the 4.1 eV luminescence in hexagonal boron nitride, Appl. Phys. Lett. **115**, 212101 (2019).

[61] F. Pinilla, W. A. Muriel, J. Cabezas-Escares, I. Chacón, C. Cardenas, and F. Munoz, Manipulating the stacking in two-dimensional hexagonal boron nitride bilayers: implications for defect-based single photon emitters, ACS Appl. Nano Mater. **7**, 6039 (2024).

[62] J. R. Reimers, A. Sajid, R. Kobayashi, and M. J. Ford, Understanding and calibrating density-functional-theory calculations describing the energy and spectroscopy of defect sites in hexagonal boron nitride, J. Chem. Theory Comput. **14**, 1602 (2018).

[63] F. Volmer, M. Ersfeld, L. Rathmann, M. Heithoff, L. Kotewitz, M. Lohmann, B. Yang, K. Watanabe, T. Taniguchi, L. Bartels *et al.*, How photoinduced gate screening and leakage currents dynamically change the fermi level in 2D materials, Phys. Status Solidi (RRL) **14**, 2000298 (2020).

[64] F.-C. Chiu, A review on conduction mechanisms in dielectric films, Adv. Mater. Sci. Eng. **2014**, 578168 (2014).

[65] L. Ju, J. Velasco, E. Huang, S. Kahn, C. Nosiglia, H.-Z. Tsai, W. Yang, T. Taniguchi, K. Watanabe, Y. Zhang, G. Zhang *et al.*, Photoinduced doping in heterostructures of graphene and boron nitride, Nat. Nanotechnol. **9**, 348 (2014).

[66] T. Liu, D. Xiang, Y. Zheng, Y. Wang, X. Wang, L. Wang, J. He, L. Liu, and W. Chen, Nonvolatile and programmable photodoping in $MoTe_2$ for photoresist-free complementary electronic devices, Adv. Mater. **30**, 1804470 (2018).

[67] D. Xiang, T. Liu, J. Xu, J. Y. Tan, Z. Hu, B. Lei, Y. Zheng, J. Wu, A. H. C. Neto, L. Liu, and W. Chen, Two-dimensional multibit optoelectronic memory with broadband spectrum distinction, Nat. Commun. **9**, 2966 (2018).

[68] C. Neumann, L. Rizzi, S. Reichardt, B. Terrés, T. Khodkov, K. Watanabe, T. Taniguchi, B. Beschoten, and C. Stampfer, Spatial control of laser-induced doping profiles in graphene on hexagonal boron nitride, ACS Appl. Mater. Interfaces **8**, 9377 (2016).

[69] S. Wang, G. Geng, Y. Sun, S. Wu, X. Hu, E. Wu, and J. Liu, Flash memory based on $MoTe_2$/boron nitride/graphene semi-floating gate heterostructure with non-volatile and dynamically tunable polarity, Nano Res. **15**, 6507 (2022).

[70] M. Abdi, J.-P. Chou, A. Gali, and M. B. Plenio, Color centers in hexagonal boron nitride monolayers: A group theory and ab initio analysis, ACS Photon. **5**, 1967 (2018).

[71] Z. Qiu, K. Vaklinova, P. Huang, M. Grzeszczyk, K. Watanabe, T. Taniguchi, K. S. Novoselov, J. Lu, and M. Koperski, Atomic and electronic structure of defects in hBN: Enhancing single-defect functionalities, ACS Nano **18**, 24035 (2024).

[72] I. Wlasny, K. Pakula, R. Stepniewski, W. Strupinski, I. Pasternak, J. M. Baranowski, and A. Wysmolek, STS observations of deep defects within laser-illuminated graphene/MOVPE-h-BN heterostructures, Appl. Phys. Lett. **114**, 102103 (2019).

[73] D. Wong, J. Velasco, L. Ju, J. Lee, S. Kahn, H.-Z. Tsai, C. Germany, T. Taniguchi, K. Watanabe, A. Zettl *et al.*, Characterization and manipulation of individual defects in insulating hexagonal boron nitride using scanning tunnelling microscopy, Nat. Nanotechnol. **10**, 949 (2015).

[74] A positive leakage current is defined for electrons flowing from the top gate to the back gate.

[75] J. Zribi, L. Khalil, J. Avila, J. Chaste, H. Henck, F. Oehler, B. Gil, S. Liu, J. H. Edgar, C. Giorgetti, Y. J. Dappe, E. Lhuillier, G. Cassabois, A. Ouerghi, and D. Pierucci, Structural and electronic transitions in few layers of isotopically pure hexagonal boron nitride, Phys. Rev. B **102**, 115141 (2020).

[76] H. Henck, D. Pierucci, G. Fugallo, J. Avila, G. Cassabois, Y. J. Dappe, M. G. Silly, C. Chen, B. Gil, M. Gatti, F. Sottile, F. Sirotti, M. C. Asensio, and A. Ouerghi, Direct observation of the band structure in bulk hexagonal boron nitride, Phys. Rev. B **95**, 085410 (2017).

[77] S. Ogawa, T. Yamada, R. Kadowaki, T. Taniguchi, T. Abukawa, and Y. Takakuwa, Band alignment determination of bulk h-BN and graphene/h-BN laminates using photoelectron emission microscopy, J. Appl. Phys. **125**, 144303 (2019).

[78] D. Pierucci, J. Zribi, H. Henck, J. Chaste, M. G. Silly, F. Bertran, P. Le Fevre, B. Gil, A. Summerfield, P. H. Beton *et al.*, van der Waals epitaxy of two-dimensional single-layer h-BN on graphite by molecular beam epitaxy: Electronic properties and band structure, Appl. Phys. Lett. **112**, 253102 (2018).

[79] T. Ouaj, L. Kramme, M. Metzelaars, J. Li, K. Watanabe, T. Taniguchi, J. H. Edgar, B. Beschoten, P. Kögerler, and C. Stampfer, Chemically detaching hBN crystals grown at atmospheric pressure and high temperature for high-performance graphene devices, Nanotechnol. **34**, 475703 (2023).

[80] T. Ouaj, C. Arnold, J. Azpeitia, S. Baltic, J. Barjon, J. Cascales, H. Cun, D. Esteban, M. Garcia-Hernandez, V. Garnier *et al.*, Benchmarking the integration of hexagonal boron nitride crystals and thin films into graphene-based van der Waals heterostructures, 2D Mater. **12**, 015017 (2025).

[81] T. Taniguchi and K. Watanabe, Synthesis of high-purity boron nitride single crystals under high pressure by using Ba–BN solvent, J. Cryst. Growth **303**, 525 (2007).

[82] J.-L. Uslu, T. Ouaj, D. Tebbe, A. Nekrasov, J. H. Bertram, M. Schütte, K. Watanabe, T. Taniguchi, B. Beschoten, L. Waldecker, and C. Stampfer, An open-source robust machine learning platform for real-time detection and classification of 2D material flakes, Mach. Learn.: Sci. Technol. **5**, 015027 (2024).

[83] L. H. Li, J. Cervenka, K. Watanabe, T. Taniguchi, and Y. Chen, Strong oxidation resistance of atomically thin boron nitride nanosheets, ACS Nano **8**, 1457 (2014).

[84] N. Khan, J. Li, and J. H. Edgar, The thermal oxidation of hexagonal boron nitride single crystals: Dry and ambient air compared, MRS Commun. **12**, 74 (2022).

[85] D. Thureja, F. E. Yazici, T. Smoleński, M. Kroner, D. J. Norris, and A. İmamoğlu, Electrically defined quantum dots for bosonic excitons, Phys. Rev. B **110**, 245425 (2024).

[86] M. Grzeszczyk, K. Vaklinova, K. Watanabe, T. Taniguchi, K. S. Novoselov, and M. Koperski, Electroluminescence from pure resonant states in hBN-based vertical tunneling junctions, Light Sci. Appl. **13**, 155 (2024).

[87] M. Onodera, K. Watanabe, M. Isayama, M. Arai, S. Masubuchi, R. Moriya, T. Taniguchi, and T. Machida, Carbon-Rich domain in hexagonal boron nitride: Carrier mobility degradation and anomalous bending of the Landau fan diagram in adjacent graphene, Nano Lett. **19**, 7282 (2019).

[88] Y. Hattori, T. Taniguchi, K. Watanabe, and K. Nagashio, Determination of carrier polarity in Fowler–Nordheim tunneling and evidence of Fermi level pinning at the hexagonal boron nitride/metal interface, ACS Appl. Mater. Interfaces **10**, 11732 (2018).

[89] G.-H. Lee, Y.-J. Yu, C. Lee, C. Dean, K. L. Shepard, P. Kim, and J. Hone, Electron tunneling through atomically flat and ultrathin hexagonal boron nitride, Appl. Phys. Lett. **99**, 243114 (2011).

[90] Y. Hattori, T. Taniguchi, K. Watanabe, and K. Nagashio, Layer-by-layer dielectric breakdown of hexagonal boron nitride, ACS Nano **9**, 916 (2015).

[91] A. Ranjan, N. Raghavan, M. Holwill, K. Watanabe, T. Taniguchi, K. S. Novoselov, K. L. Pey, and S. J. O'Shea, Dielectric breakdown in single-crystal hexagonal boron nitride, ACS Appl. Electron. Mater. **3**, 3547 (2021).

[92] J. Cao, M. Tian, S. Zhang, W. Hu, N. Wan, and T. Lin, Carbon-related defect control of bulk hBN single crystals growth by atmospheric-pressure metal-flux-based fusion synthesis, J. Mater. Sci. **57**, 14668 (2022).

[93] H. Yamada, S. Inotsume, N. Kumagai, T. Yamada, and M. Shimizu, Comparative study of boron precursors for chemical vapor-phase deposition-grown hexagonal boron nitride thin films, Phys. Status Solidi (A) **218**, 2000241 (2021).

[94] A. Perepeliuc, R. Gujrati, A. Srivastava, P. Vuong, V. Ottapilakkal, P. L. Voss, S. Sundaram, J. P. Salvestrini, and A. Ougazzaden, Photoinduced doping in hexagonal boron nitride, Appl. Phys. Lett. **122**, 263503 (2023).

[95] Y. Y. Illarionov, T. Knobloch, M. Jech, M. Lanza, D. Akinwande, M. I. Vexler, T. Mueller, M. C. Lemme, G. Fiori, F. Schwierz, and T. Grasser, Insulators for 2D nanoelectronics: The gap to bridge, Nat. Commun. **11**, 3385 (2020).

[96] Y. Y. Illarionov, G. Rzepa, M. Waltl, T. Knobloch, A. Grill, M. M. Furchi, T. Mueller, and T. Grasser, The role of charge trapping in MoS_2/SiO_2 and MoS_2/hBN field-effect transistors, 2D Mater. **3**, 035004 (2016).

[97] P. Tamarat, T. Gaebel, J. R. Rabeau, M. Khan, A. D. Greentree, H. Wilson, L. C. L. Hollenberg, S. Prawer, P. Hemmer, F. Jelezko, and J. Wrachtrup, Stark shift control of single optical centers in diamond, Phys. Rev. Lett. **97**, 083002 (2006).

[98] W. Albrecht, J. Moers, and B. Hermanns, HNF-Helmholtz nano facility, JLSRF **3**, A112 (2017).

[99] A. Kurzmann *et al.*, data and analysis scripts for "Current-induced brightening of dark vacancy emitters in hexagonal boron nitride" Zenodo (2025), doi:10.5281/zenodo.14049616.